Research Article

Journal of PeptideScience

Received: 14 May 2010 Revised: 23 July 2010 Accepted: 29 July 2010 Published online in Wiley Online Library: 17 September 2010

(wileyonlinelibrary.com) DOI 10.1002/psc.1293

Improved Fmoc-based solid-phase synthesis of homologous peptide fragments of human and mouse prion proteins

Dolors Grillo-Bosch,[a,b] Francesc Rabanal[b] and Ernest Giralt[a,b]*

The synthesis of difficult peptide sequences has been a challenge since the very beginning of SPPS. The self-assembly of the growing peptide chains has been proposed as one of the causes of this synthetic problem. However, there is an increasing need to obtain peptides and proteins that are prone to aggregate. These peptides and proteins are generally associated with diseases known as *amyloidoses*. We present an efficient SPPS of two homologous peptide fragments of HuPrP (106–126) and MoPrP105–125 based on the use of the PEGA resin combined with proper coupling approaches. These peptide fragments were also studied by CD and TEM to determine their ability to aggregate. On the basis of these results, we support PEG-based resins as an efficient synthetic tool to prepare peptide sequences prone to aggregate on-resin. Copyright © 2010 European Peptide Society and John Wiley & Sons, Ltd.

Keywords: difficult sequence; prion protein; aggregation; PEGA resin

Introduction

An inherent problem in stepwise SPPS is the self-association of the growing peptide chains [1], which can lead to incomplete coupling and/or deprotection reactions [2]. Peptide sequences that present this problem have been commonly known as *difficult sequences* [3]. One cause of these undesired synthetic problems is the self-association of the growing peptide chain in β-sheets [4–7].

There is an ever-increasing need for synthetic peptides and proteins that are associated with the diseases known as *amyloidoses*, which include AD, PD, and prion diseases such as CJD. In amyloidoses, specific peptides or proteins fail to fold or to remain correctly folded, and then aggregate into amyloid deposits [8]. These deposits contain amyloid fibrils that exhibit a cross-β structure composed of β-sheets of the peptide where the β-strands run nearly perpendicular to the long axis of the fibril and the interchain hydrogen bonds run nearly parallel to the long axis of the fibril [9,10]. Owing to their high tendency to aggregate, these peptides and proteins are difficult to synthesise by chemical solid-phase methods [11,12].

The key event in the pathogenesis of prion diseases is the conformational change of normal cellular prion protein (PrP^{C}) to the infectious, protease-resistant prion (PrP^{Sc}) form, which aggregates into amyloid fibrils [13–15]. PrP^{C} is an extracellular glycoprotein containing a hydrophobic path within residues 113–128 that is highly conserved among all studied species [16,17]. Peptide fragments containing all or part of this region have been used as models for PrP aggregation *in vitro* [18,19]. These fragments include a frequently used one that spans residues 106–126 of HuPrP, known as *HuPrP106–126* (Figure 1(a)), which contains a group of hydrophilic amino acids at its *N*-terminus (^{106}KTNMKH^{112}M) and hydrophobic amino acids at its *C*-terminus (^{113}AGAAAAGAVVGGL^{126}G) [18,20,21]. HuPrP106–126 has been described to exhibit some of the physicochemical and pathogenic properties of PrP^{Sc}. It has a high tendency to adopt a β-sheet secondary structure [22], forms amyloid fibrils *in vitro* [23,] is partially resistant to proteolysis [24], and is toxic to neurons *in vitro* [23,25]. These qualities make HuPrP106–126 a good candidate for modelling the aggregation or inhibition of PrP. However, HuPrP106–126 is also considered to be a difficult synthetic target because of its high tendency to aggregate [26].

Various stepwise SPPSs of HuPrP106–126 using either Boc or Fmoc strategies have been reported. Although the Boc-based ones have proven to be successful [26], the Fmoc-based ones have offered varying levels of success [26–29]. In general, the Fmoc-based syntheses use polystyrene resins, such as the Wang resin, and differ in their approach in resolving undesired self-association of the growing sequence, encompassing the use of Hmb-amide protecting groups [26,27,] Dmb-protected dipeptides [29], a mixture of DMF/NMP as solvent [30], and/or high temperatures [28,31]. However, using extreme conditions

* *Correspondence to: Ernest Giralt, Institute for Research in Biomedicine, Barcelona Science Park, Baldiri Reixac 10, E-08028 Barcelona, Spain. E-mail: ernest.giralt@irbbarcelona.org*

a *Institute for Research in Biomedicine, Barcelona Science Park, Baldiri Reixac 10, E-08028 Barcelona, Spain*

b *Department of Organic Chemistry, University of Barcelona, Martí i Franquès 1-11, E-08028 Barcelona, Spain*

Abbreviations used: *AD, Alzheimer's disease; tBu, tert-butyl; CJD, Creutzfeldt-Jakob disease; DIPCDI, N′,N″-diisopropylcarbodiimide; EDT, 1,2-ethanedithiol; f_i, initial functionalisation; 4-HCCA, α-cyano-4-hydroxycinnamic acid; HMBA, 4-hydroxymethylbenzoic acid; HuPrP, human prion protein; PD, Parkinson's disease; PrP, prion protein; MeCN, acetonitrile; MoPrP, mouse prion protein; NMP, N-methyl-2-pyrrolidone; TEM, transmission electron microscopy; ThT, thioflavine T; TIS, triisopropylsilane; TOF, time of flight. Amino acid symbols denote the L configuration unless otherwise stated. All reported solvent ratios are expressed as volume/volume unless otherwise indicated.*

Journal of PeptideScience

(a) ^{106}K-T-N-M-K-H-M-A-G-A-A-A-A-G-A-V-V-G-G-L-G^{126} HuPrP(106-126)

(b) ^{105}K-T-N-L-K-H-V-A-G-A-A-A-A-G-A-V-V-G-G-L-G^{125} MoPrP(105-125)

Figure 1. Sequences of the synthesised PrP fragments. The hydrophilic amino acids of the *N*-terminal section are shown in black, the hydrophobic amino acids of the *C*-terminal section are shown in blue, and the amino acids that differ between HuPrP and MoPrPs in these peptide fragments are shown in red. (a) HuPrP fragment spanning residues 106–126 (HuPrP). (b) The homologous MoPrP fragment, containing residues 105–125 (MoPrP).

for amino acid couplings – especially high temperatures – can decrease the quality of the desired peptide, chiefly due to side reactions such as amino acid racemisation [1].

Herein we present efficient solid-phase syntheses of both HuPrP106–126 (Figure 1(a)) and its homologue MoPrP fragment, which spans residues 105–125 of MoPrP (Figure 1(b)), on PEGA resin. Although this hydrophilic copolymer resin was originally described by Meldal *et al*. as a convenient support for post-synthetic screening of peptides in aqueous environments – including for assays entailing large biomolecules (e.g. enzymes or other proteins) [32–34] – , we found that it also performs very well for synthesising peptide sequences prone to self-associate on-resin.

Materials and Methods

Reagents and Solvents

Fmoc-protected amino acids were obtained from Advanced ChemTech (Louisville, KY, USA), Iris Biotech GmbH (Marktredwitz, Germany) and Senn Chemicals (Dielsdorf, Switzerland). Coupling agents such as TBTU and HOBt were purchased from Albatros Chem. Inc. (Montreal, Canada); DIPCDI and DMAP were acquired from Fluka (Buchs, Switzerland); and DIEA was supplied by Merck (Hohenbrunn, Germany). HMBA was obtained from Novabiochem (Läufelfingen, Switzerland) and PEGA resin from Polymer Laboratories (Shropshire, UK). Solvents such as TFA were acquired from Fluorochem (Old Glossop, UK) and piperidine, toluene, DMF, DCM, and MeCN from SDS (Peypin, France). DBU was purchased from Aldrich (Steinhein, Germany). Scavengers like EDT was acquired from Aldrich (Milwaukee, WI, USA) and TIS from Fluka (Buchs, Switzerland). MilliQ water was obtained using a MilliQ gradient A10 system (Millipore, Billerica, MA, USA). 4-HCCA was purchased from Aldrich (Steinhein, Germany). NaOH was supplied by Sigma–Aldrich Co. (St. Louis, MO, USA). HCl was purchased from Scharlau (Barcelona, Spain). ThT was obtained from Fluka (Buchs, Switzerland) and uranyl acetate from Electron Microscopy Sciences (Fort Washington, PA, USA). Finally, all Edman degradation reagents were purchased from Applied Biosystems (Foster City, CA, USA).

Peptide Synthesis

Peptides were synthesised at a 100-µmol scale. HMBA handle was manually coupled to PEGA resin (f_i = 0.4 mmol/g; particle size = 300–500 µm) using HMBA/TBTU/DIEA (3 : 2.85 : 6 equiv. with respect to the resin). HMBA, TBTU, and DIEA were dissolved in 1 ml DMF, and, after 3 min of preactivation, this mixture was added to the resin. A few drops of DCM were added to favour resin swelling. The reaction was then stirred for 4 h at 315 rpm using an orbital shaker [34]. Total coupling was estimated by the Kaiser test [35].

The first amino acid, Fmoc-Gly-OH, was also coupled manually. Fmoc-Gly-OH/DIPCDI/DMAP (4 : 4 : 0.4) were dissolved in 1 ml DMF, and, after 3 min of preactivation, this mixture was added to the resin. A few drops of DCM were added to favour resin swelling. The reaction was stirred for 1 h at 315 rpm using an orbital shaker. An additional cycle of coupling was required for complete incorporation of Fmoc-Gly-OH. Total coupling was determined by the alcohol test [36].

The rest of the amino acids were assembled by automated Fmoc solid-phase synthesis using an Applied Biosystems model 433A peptide synthesiser (Foster City, CA, USA) following the FastMoc 0.10 ΩmonPrev PK method [37]. Briefly, Fmoc groups were removed using piperidine/DMF (1 : 4) by means of two short deprotection cycles (2 min × 2 min) and one long cycle (7.6 min). After a cleaning step with DMF (4 min × 2.5 min), the amino acids were dissolved in the appropriate volume of 0.45 M TBTU/HOBt in DMF for 7.6 min followed by the addition of the appropriate volume of 2 M DIEA in NMP to activate the amino acid and transfer it to the reactor (2.1 min). Couplings (13.8 min) were mediated by TBTU/HOBt/DIEA (9 : 9 : 20 equiv. with respect to the resin) using 10 equiv. of Fmoc-amino acids. Finally, the side-chain-protecting groups of HuPrP106–126 and MoPrP105–125 were removed with TFA/H_2O/EDT/TIS (94 : 2.5 : 2.5 : 1) for 2 h and TFA/H_2O/TIS (95 : 2.5 : 2.5) for 1 h, respectively, with mild orbital shaking. If needed, peptides were cleaved from the resin using aq. 0.1 M NaOH for 2 h. Finally, the cleavage mixture was treated with 0.1 M aq. HCl until it reached neutral pH.

Peptide Characterisation and Quantification

Peptides were characterised by analytical RP–HPLC [Waters 2695 separation module equipped with a 996 PDA (Waters, Massachusetts, USA), and a reverse-phase symmetry column (C18, 5 µm, 4.6 × 150 mm, Waters); flow = 1 ml/min; linear gradient: 0–40% B in 15 min (A = 0.045% TFA in H_2O; B = 0.036% TFA in MeCN), detection at λ = 220 nm].

Peptide identities were confirmed by MALDI–TOF mass spectra analysis (Applied Biosystems 4700 proteomics analyser); HPLC–MS [Waters 2795 separation module equipped with a Waters 2487 dual λ absorbance detector; Waters ESI–MS micromass ZQ detector; reverse-phase Symmetry® column (C18, 4.6 mm × 150 mm, 5 µm, Waters)]; and Edman degradation (Procise CLC^{492} Applied Biosystem module, Foster City, CA). The matrix used for sample analysis by MALDI–TOF was a saturated solution of 4-HCCA in 1 : 1 MeCN/H_2O with 0.05% TFA.

Peptides were quantified by amino acid analysis on a Beckman System 6300 equipped with a 250 mm × 4 mm cation exchange column of polysulphonate resin after being hydrolysed in 6 M aq. HCl at 110 °C for 24 h.

Peptide Purification

Crude peptides were purified by semi-preparative RP–HPLC [Waters 600 controller equipped with Waters 2487 dual λ absorbance detector, and a symmetry column (C8, 5 µm, 30 mm × 100 mm, Waters); flow = 10 ml/min; gradient = 0% B for 5 min, then 0–10% B in 5 min, then 10–50% B in 30 min (A = 0.1% TFA in H_2O; B = 0.1% TFA in MeCN), detection at λ = 220 nm].

Preparation of PrP Fragments for Aggregation Assays

Stock solutions (1 mM) of HuPrP106–126 and of MoPrP105–125 in MilliQ H_2O at 4 °C were prepared. Samples were spun down (Eppendorf 5415 R centrifuge) at 10 000 rpm for 10 min at 4 °C to remove aggregates. The exact concentration was determined by amino acid analysis, and the desired amounts of these stock solutions were then taken and lyophilised. The lyophilised samples were dissolved in 140 mM KF, 10 mM potassium phosphate buffer (pH 7.41) to obtain a final concentration of 537 μM. Both peptide samples were left to aggregate to generate amyloid fibrils.

Electron Microscopy

Fibril formation was tracked by TEM using the drop method. Briefly, 10 μl of sample were applied to formvar-coated carbon grids (400 mesh) for 1 min. The grid with the sample was then washed with two drops of MilliQ H_2O (1 min/drop). Finally, the grid was negatively stained with two drops (40 μl each) of 2% aqueous uranyl acetate. The samples were air dried, and then viewed in a JEOL JEM (Tokyo, Japan) 1010 TEM, operating at 80 KV and equipped with a MegaView III digital camera from SoftImaging (Münster, Germany). The software used was the analysis from SoftImaging (Münster, Germany).

Circular Dichroism

All CD measurements were taken with a JASCO J-810 spectropolarimeter and Hellma 1 mm light-path precision cells made of suprasil quartz. CD data were analysed using spectra analysis v. 1.53.04 software.

CD samples were prepared as follows: briefly, 2.1 mg of HuPrP106–126 and 1.9 mg of MoPrP105–125, determined by amino acid analysis, were dissolved in 2000 and 1750 μl of MilliQ H_2O respectively. Aliquots were taken and lyophilised. Each aliquot was dissolved in the appropriate volume of 140 mM KF and 10 mM phosphate buffer (pH 7.41) to obtain 537 μM peptide solutions.

CD measurements on the PrP fragments were taken at 0 and 24 h, 4 and 6 days after the start of aggregation. Aggregated samples were left on a VorTemp 56 benchtop incubator at 500 rpm at 27 °C. After the appropriate aggregation period, 80 μl aliquots of each solution were taken, and then stored at 4 °C until measurement. Prior to measurement, each sample was diluted in MilliQ H_2O at 1 : 4 (v/v).

Results and Discussion

Peptide Synthesis and Characterisation

We chose our synthetic approach based on the high content of hydrophobic amino acids at the *C*-terminus of HuPrP106–126 and MoPrP105–125 (Figure 1), as we aimed to minimise on-resin peptide self-assembly during synthesis, in order to avoid formation of any deletion peptides. Although Boc/Bzl strategy is sometimes recommended for difficult sequences due to the repetitive use of TFA that can prevent on-resin aggregation of the growing peptide chain, we selected instead a combination of Fmoc/tBu chemistry and a polar resin, such as PEGA, to explore other approaches to avoid this problem. Fmoc/tBu chemistry had been previously reported to be successful to obtain HuPrP106–126 [29]. However, Cardona *et al*. use polystyrene Wang resin combined with Dmb-peptides and single 30-min coupling reactions. In our case, we chose the PEGA resin, composed of a hydrophilic copolymer because it has better swelling properties – including in aqueous solvents [34] – compared to the Wang resin, which is polystyrene based. In addition, it also avoids protected peptide–resin interaction because of its polar nature [12,38]; features a low to medium level of functionalisation; is also amenable to automated peptide synthesis; is highly flexible, owing to its internal structure [32,33]; and, lastly, is compatible with biological assays [32,39,40]. We selected HMBA as the handle, owing to its stability to TFA, which ensures an adequate protection scheme. Moreover, using this handle the cleavage can be performed with a variety of nucleophiles to generate peptides with various *C*-terminal carboxy modifications [41,42]. We used 0.1 M aq. NaOH to release the peptides as their *C*-terminal free carboxylic acids.

Our first synthesis of peptide HuPrP106–126 gave a poor yield (49%) and contained many impurities (purity $\leq$39%) (Figure 2(a)). Deletions of Lys^{106}, Thr^{107}, His^{111}, and Ala^{115} were detected by Edman degradation and MALDI–TOF MS (Figure 2(a)). Thus, for subsequent syntheses, we employed systematic recouplings in these positions. We also introduced extra systematic recouplings in positions that we considered as potentially prone to deletions (Ala^{116} and Val^{121}).

The second synthesis of HuPrP106–126, using the new protocol (Figure 2(b)), gave a crude product of much higher purity (>74%) and in better yield (63%). HPLC and MALDI–TOF MS analyses (Figure 2(b)) revealed minor amounts of other, more hydrophilic peptides, which we were unable to identify. The MALDI–TOF MS spectrum confirmed the expected product [$(M+H)^+$, m/z = 1911.9] and also showed peaks corresponding to adducts $(M+Na)^+$ (m/z = 1933.9) and $(M+K)^+$ (m/z = 1955.9).

The crude peptide was lyophilised and purified by semi-preparative HPLC (Figure 2(c)). We obtained aliquots of HuPrP106–126 of >92% purity, which were characterised by HPLC, amino acid analysis, and mass spectrometry (Figure 2(c)). HPLC revealed a single peak (r_t = 9.97 min) and the mass spectrum confirmed the presence of the $(M+H)^+$ species (m/z = 1911.9) corresponding to the desired molecule, HuPrP106–126, together with the $(M+Na)^+$ (m/z = 1933.9) and $(M+K)^+$ (m/z = 1949.9) peaks.

The results obtained using this protocol equal [29] or improve [26] the ones reported previously by other groups using Fmoc strategy. These last groups were not able to obtain the peptide or obtained the crude peptide in very poor yield (under 10%) [26].

Taking into account these results, we then synthesised MoPrP105–125 using the recouplings established for HuPrP106–126. The first crude peptide of MoPrP105–125 showed a purity higher than 80% (Figure 3(a)) and was obtained in an overall yield of 68%. In its MALDI–TOF spectrum, apart from the peaks corresponding to the mass of the desired peptide [$(M+H)^+$, $(M+Na)^+$, and $(M+K)^+$], we also identified a peak corresponding to $(M+Trt)^+$ (Figure 3(a)), which resulted from incomplete cleavage of the protecting group of the Asn and/or His residues. However, complete cleavage was achieved by simply increasing the cleavage time. We also observed a $(M-18+H)^+$ (m/z = 1843.7) peak, which may indicate neutral loss of a water molecule possibly from Thr. This loss may have been induced by the high intensity laser used to ionise the sample [43]. Finally, we also observed minor peaks correlating to peptide fragments that correspond to single amino

Journal of PeptideScience

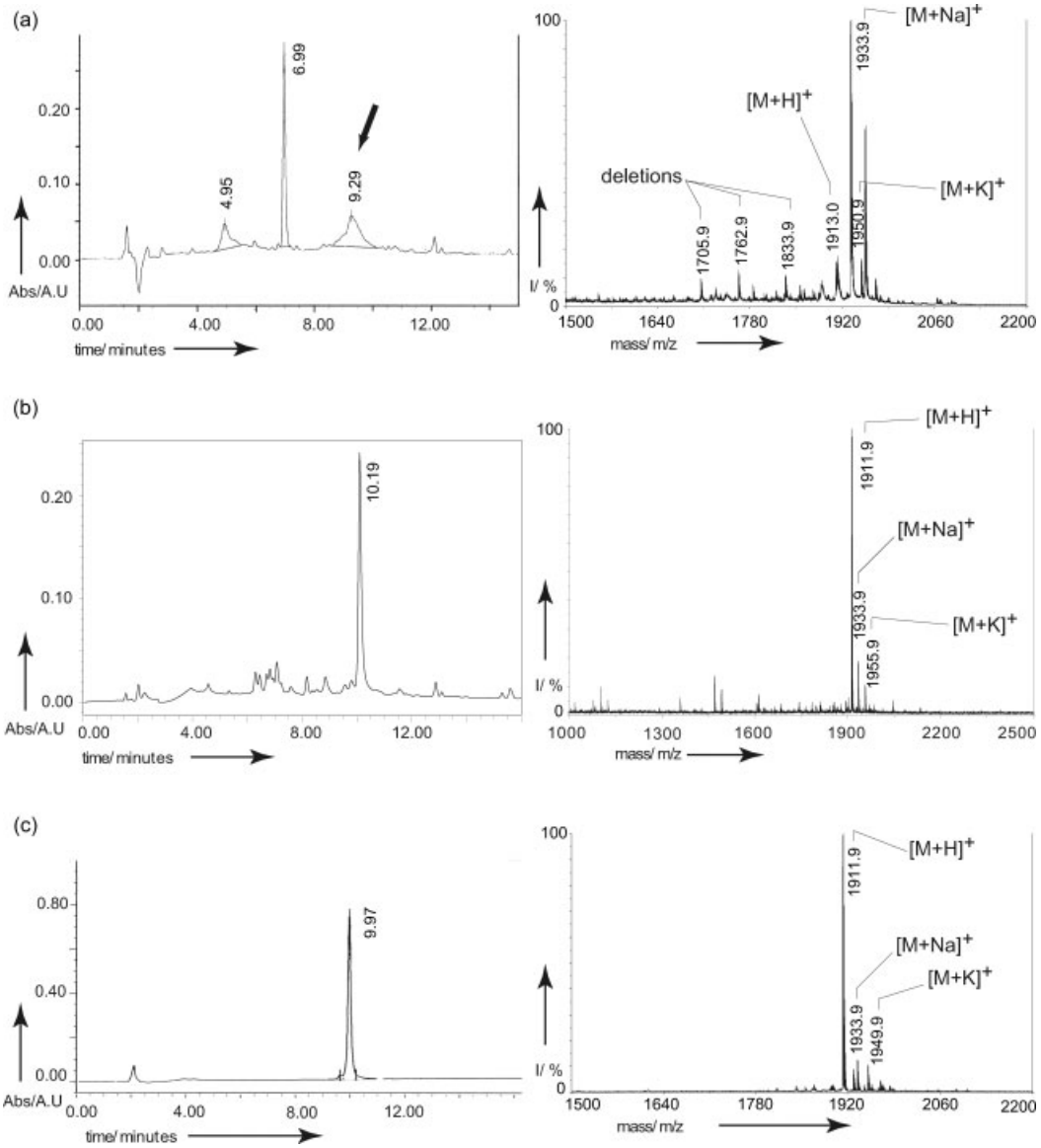

Figure 2. HPLC chromatograms and MALDI-TOF mass spectra of synthesised HuPrP106–126 before and after purification. HPLC was run using linear gradients of B in A (A = H_2O with 0.045% TFA; B = MeCN with 0.036% TFA), and detection at 220 nm. All the MALDI-TOF spectra show the expected product [$(M+H)^+$] and the peaks corresponding to adducts $(M+Na)^+$ and $(M+K)^+$. (a) Characterisation of the first synthesis. The chromatogram of the crude product was obtained using a linear gradient: 5–40% B in A. The peak correlating to the expected peptide is marked with an arrow. The MALDI-TOF spectrum of the crude product also shows lower *m/z* peaks. (b) Characterisation of the second synthesis. The HPLC profile of the crude product was obtained using a linear gradient: 0–40% B in A. (c) Characterisation of purified HuPrP106–126. HPLC profile of the pure product obtained using a linear gradient: 0–40% B in A.

acid deletions of Val, Gly, or Ala (Figure 3(a)). All these amino acids are located at the *C*-terminal region, which synthetically is the most challenging one.

Finally, we purified MoPrP105–125 by semi-preparative HPLC. We obtained a peptide with purity higher than 90%. Its MALDI-TOF spectrum confirmed the expected molecular weight and high purity of MoPrP105–125. The $(M+H)^+$ (m/z = 1862.0), $(M+Na)^+$ (m/z = 1884.0), $(M+K)^+$ (m/z = 1899.9), and $(M+Na+K)^+$ (m/z = 1921.9) peaks were detected almost exclusively.

In summary, our results, when compared to the ones of Cardona *et al*., suggest that, to prepare aggregation-prone sequences by Fmoc/*t*But SPPS without the use of backbone protection (Dmb), a polar support and recouplings at difficult positions are required. Thus, both approaches are reasonable and appropriate.

Peptide Aggregation Assays

As mentioned in the preceding paragraph, amyloid fibrils exhibit a cross-β structural motif formed by β-sheets [9,10]. Thus, to study the ability of each peptide fragment to form amyloid fibrils, we used CD to evaluate the presence of β-sheets as this technique has proven useful for determining the secondary structure of proteins in solution [44–47]. Finally, we used TEM to assess the morphology of the aggregates.

We studied the secondary structural changes of both peptide fragments, HuPrP106–126 and MoPrP105–125, by CD at a concentration of 537 μM for 6 days. For HuPrP106–126, we initially observed a strong negative band at 196 nm, which suggested that the dominant structure present was a random coil, and a weak negative band near 225 nm, which had previously been

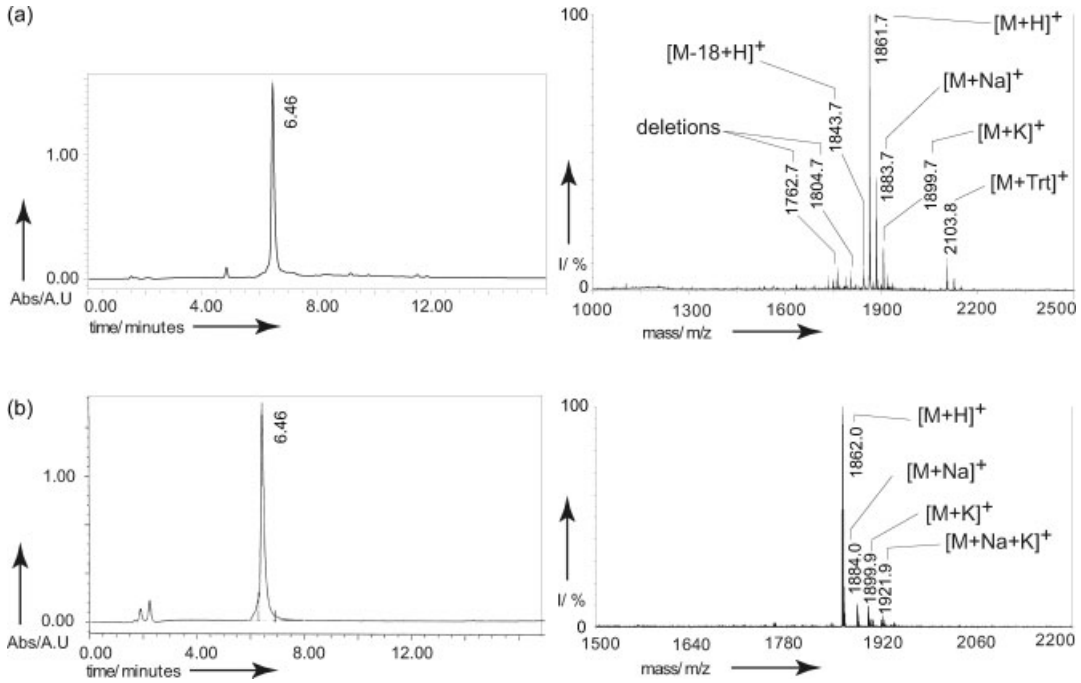

Figure 3. HPLC chromatograms and MALDI-TOF mass spectra of synthesised MoPrP105–125 before and after purification. HPLC was run using linear gradients of 10–50% of B in A (A = H_2O with 0.045% TFA; B = MeCN with 0.036% TFA), and detection at 220 nm. (a) HPLC chromatogram of crude MoPrP105–125. The MALDI-TOF MS spectrum contains the expected masses [$(M+H)^+$, $(M+Na)^+$ and $(M+K)^+$], plus higher [$(M+Trt)^+$] and lower [$(M-18+H)^+$] and deletions peaks. (b) HPLC chromatogram of purified MoPrP105–125. The MALDI-TOF mass spectrum of the purified peptide shows the expected masses [$(M+H)^+$, $(M+Na)^+$, $(M+K)^+$ and $(M+Na+K)^+$].

attributed to the presence of small amounts of β-sheet [28] (Figure 4(a)). After 24 h of aggregation, we observed a very intense positive band centred at 197 nm and a strong negative band at 220 nm (Figure 4(a)), both of which are characteristic of β-sheet structures. After 4 days of incubation, the intensity of both bands decreased, but after 6 days, it plateaued, suggesting that some of the structures had precipitated out of solution (Figure 4(a)).

For MoPrP105–125, we initially observed a broad negative band centred at 197 nm, which is indicative of a random coil structure (Figure 4(b)). After 24 h of aggregation we observed a maximum centred at 212 nm that we interpreted as a transition band between the initial random coil structure and the final secondary structure (Figure 4(b)). After 4 days of incubation, we observed the characteristic β-sheet bands, with a maximum centred at 199 nm and a broad negative band centred at 219 nm. After 6 days of incubation, the intensity of both bands had decreased and the maximum had shifted slightly, towards 201 nm (Figure 4(b)), possibly indicating that some of the structures had precipitated out of solution.

We also followed the aggregation process of both peptide fragments by TEM for 6 days. For HuPrP106–126, we initially observed doughnut-like protofibrils [48,49] together with very short fibrils (Figure 4(a)). After 24 h, we observed amyloid fibrils, which is in agreement with the CD results of a strong band suggesting a β-sheet. At 4 and 6 days of incubation, we observed only thin, unbranched amyloid fibrils similar to the ones reported previously [50] (Figure 4(a)).

Similarly, for MoPrP105–125, we initially observed doughnut-like protofibrils together with amorphous material and some fibrils (Figure 4(b)). After 24 h of incubation we observed unbranched amyloid fibrils with lateral stacking. At 4 days of incubation, we similarly observed unbranched amyloid fibrils with lateral stacking together with some circular protofibrils. Finally, at 6 days of incubation, only the presence of unbranched amyloid fibrils with lateral stacking could be observed.

These TEM results are consistent with the CD results and indicate that both peptide fragments can form amyloid fibrils under the selected conditions.

Conclusions

In summary, we have presented a highly efficient solid-phase synthesis of hydrophobic, alanine-rich peptide fragments of HuPrP and MoPrPs, which is based on Fmoc/*t*Bu chemistry. We used a combination of PEGA resin with appropriate systematic recouplings. The moderate functionalisation together with the swelling properties of polar PEGA resin probably contribute to minimising on-resin self-association and interaction with the resin of growing peptide chains when synthesised by SPPS. Finally, as expected, the synthesised PrP peptide fragments were observed to form amyloid fibrils, as assessed by CD and TEM. In light of our results, we conclude that PEG-based resins in combination with an optimised coupling strategy have proven to be an efficient synthetic tool that yields peptides containing difficult sequences prone to aggregate in high yield and purities.

Acknowledgements

The authors thank Dr Carmen López-Iglésias (SCT-UB) for technical advice on TEM, Dr Alberto Adeva (SCT-UB) for technical assistance on peptide synthesis, and Dr Eliandre Oliveira (SCT-UB) for technical support on Edman degradation. This work was supported by MEC-FEDER (BIO2008-00799, CTQ2008-06200) and Generalitat de Catalunya (XRB and Grups Consolidats 2009SGR1005).

Journal of PeptideScience

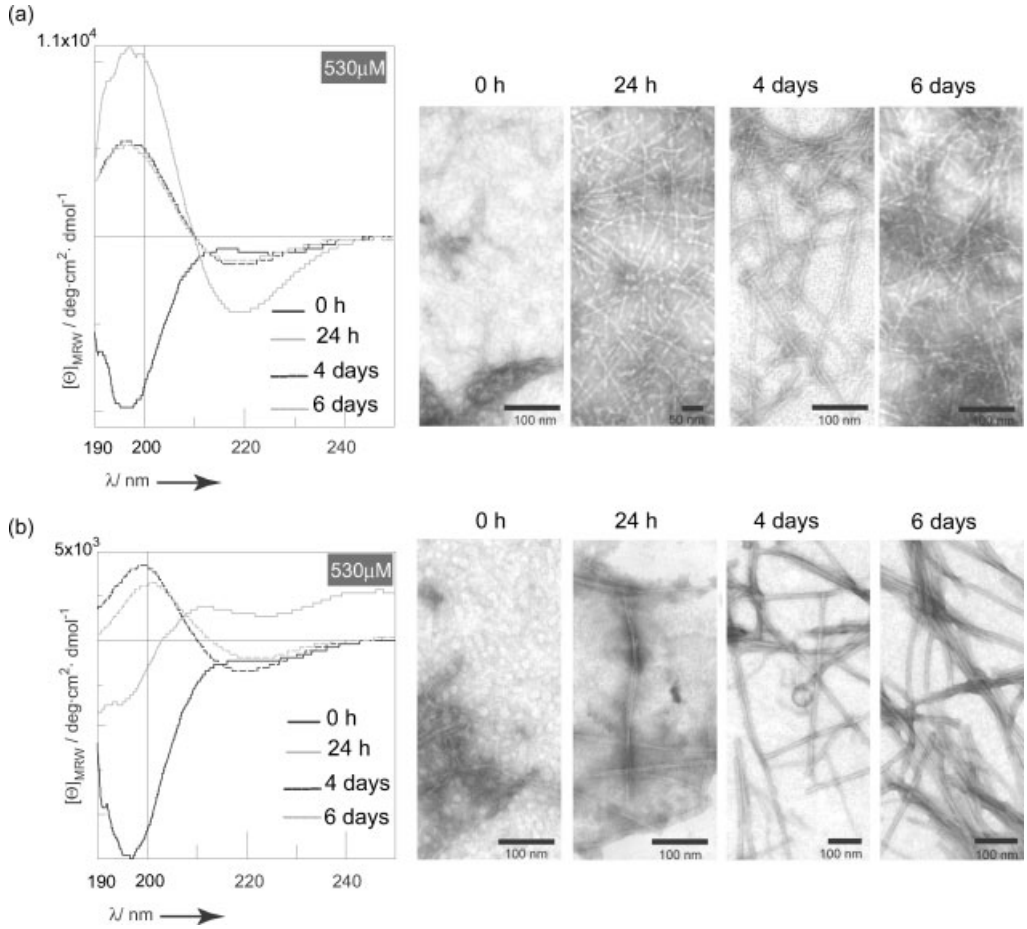

Figure 4. CD spectra and TEM micrographies obtained for synthesised homologous fragments of HuPrP and MoPrPs at 530 μM. Each CD panel contains four spectra that were recorded at different time points of aggregation: 0 h (black solid line) and 24 h (grey solid line); 4 days (black dashed line) and 6 days (grey dashed line). Each spectrum represents two independent experiments. TEM micrographies of the samples analysed by CD at different time points are: 0 and 24 h; 4 and 6 days. (a) CD spectra and TEM micrographies of HuPrP106–126. (b) CD spectra and TEM micrographies of MoPrP105–125.

References

1 Lloyd-Williams PA, Albericio F, Giralt E. *Chemical Approaches to the Synthesis of Peptides and Proteins*. CRC Press: Boca Raton, New York, 1997.
2 Merrifield RB. Solid phase peptide synthesis. I. The synthesis of a tetrapeptide. *J. Am. Chem. Soc.* 1963; **85**: 2149–2154.
3 Kent SBH. Difficult sequences in stepwise peptide synthesis: common molecular origins in solution and solid phase? *Pept.: Struct. Funct., Proc. Am. Pept. Symp. 9th* 1985; 407–414.
4 Live DH, Kent SBH. Correlation of coupling rates with physicochemical properties of resin-bound peptides in solid phase synthesis. *Pept.: Struct. Funct., Proc. Am. Pept. Symp, 8th* 1983; 65–68.
5 Ludwick AG, Jelinski LW, Live D, Kintanar A, Dumais JJ. Association of peptide chains during Merrifield solid-phase peptide synthesis. A deuterium NMR study. *J. Am. Chem. Soc.* 1986; **108**: 6493–6496.
6 Mutter M, Oppliger H, Zier A. Solubilizing protecting groups in peptide synthesis. Effect of side-chain-attached polyethylene glycol derivatives upon beta-sheet formation of model peptides. *Makromol. Chem., Rapid Commun.* 1992; **13**: 151–157.
7 Pudelko M, Kihlberg J, Elofsson M. Application of gel-phase 19F NMR spectroscopy for optimization of solid-phase synthesis of a hydrophobic peptide from the signal sequence of the mucin MUC1. *J. Pept. Sci.* 2007; **13**: 354–361.
8 Stefani M, Dobson CM. Protein aggregation and aggregate toxicity: new insights into protein folding, misfolding diseases and biological evolution. *J. Mol. Med.* 2003; **81**: 678–699.
9 Sunde M, Blake C. The structure of amyloid fibrils by electron microscopy and X-ray diffraction. *Adv. Protein Chem.* 1997; **50**: 123–159.
10 Tycko R. Molecular structure of amyloid fibrils: insights from solid-state NMR. *Q. Rev. Biophys.* 2006; **39**: 1–55.
11 Sohma Y, Hayashi Y, Kimura M, Chiyomori Y, Taniguchi A, Sasaki M, Kimura T, Kiso Y. The 'O-acyl isopeptide method' for the synthesis of difficult sequence-containing peptides: application to the synthesis of Alzheimer's disease-related amyloid beta peptide (A-beta) 1–42. *J. Pept. Sci.* 2005; **11**: 441–451.
12 Garcia-Martin F, Quintanar-Audelo M, Garcia-Ramos Y, Cruz LJ, Gravel C, Furic R, Cote S, Tulla-Puche J, Albericio F. ChemMatrix, a poly(ethylene glycol)-based support for the solid-phase synthesis of complex peptides. *J. Comb. Chem.* 2006; **8**: 213–220.
13 Hope J. Prions and neurodegenerative diseases. *Curr. Opin. Genet. Dev.* 2000; **10**: 568–574.
14 Cummings JL. *The Neuropsychiatry of Alzheimer's Disease and Related Dementias*. Martin Dunitz Ltd., Taylor and Francis group: London, 2003.
15 Soto C, Estrada Lisbell D. Protein misfolding and neurodegeneration. *Arch. Neurol.* 2008; **65**: 184–189.
16 Huang Z, Gabriel JM, Baldwin MA, Fletterick RJ, Prusiner SB, Cohen FE. Proposed three-dimensional structure for the cellular prion protein. *Proc. Natl. Acad. Sci. USA* 1994; **91**: 7139–7143.
17 Schatzl HM, Da Costa M, Taylor L, Cohen FE, Prusiner SB. Prion protein gene variation among primates. *J. Mol. Biol.* 1995; **245**: 362–374.
18 Forloni G, Tagliavini F, Bugiani O, Salmona M. Amyloid in Alzheimer's disease and prion-related encephalopathies: studies with synthetic peptides. *Prog. Neurobiol.* 1996; **49**: 287–315.
19 Brown DR. Prion protein peptides: optimal toxicity and peptide blockade of toxicity. *Mol. Cell. Neurosci* 2000; **15**: 66–78.

20 Kourie JI, Culverson A. Prion peptide fragment PrP[106–126] forms distinct cation channel types. *J. Neurosci. Res.* 2000; **62**: 120–133.
21 Kanapathipillai M, Ku SH, Girigoswami K, Park CB. Small stress molecules inhibit aggregation and neurotoxicity of prion peptide 106–126. *Biochem. Bioph. Res. Co.* 2008; **365**: 808–813.
22 De Gioia L, Selvaggini C, Ghibaudi E, Diomede L, Bugiani O, Forloni G, Tagliavini F, Salmona M. Conformational polymorphism of the amyloidogenic and neurotoxic peptide homologous to residues 106–126 of the prion protein. *J. Biol. Chem.* 1994; **269**: 7859–7862.
23 Tagliavini F, Prelli F, Verga L, Giaccone G, Sarma R, Gorevic P, Ghetti B, Passerini F, Ghibaudi E, Forloni G, Salmona M, Bugiani O, Frangione B. Synthetic peptide homologous to prion protein residues 106–147 form amyloid-like fibrils in vitro. *Proc. Natl. Acad. Sci. USA* 1993; **90**: 9678–9682.
24 Selvaggini C, De Gioia L, Cantu L, Ghibaudi E, Diomede L, Passerini F, Forloni G, Bugiani O, Tagliavini F, Salmona M. Molecular characteristics of a protease-resistant, amyloidogenic and neurotoxic peptide homologous to residues 106–126 of the prion protein. *Biochem. Bioph. Res. Co.* 1993; **194**: 1380–1386.
25 Forloni G, Angeretti N, Chiesa R, Monzani E, Salmona M, Bugiani O, Tagliavini F. Neurotoxicity of a prion protein fragment. *Nature* 1993; **362**: 543–546.
26 Jobling MF, Barrow CJ, White AR, Masters CL, Collins SJ, Cappai R. The synthesis and spectroscopic analysis of the neurotoxic prion peptide 106–126: comparative use of manual Boc and Fmoc chemistry *Lett. Pept. Sci.* 1999; **6**: 129–134.
27 Hyde C, Johnson T, Owen D, Quibell M, Sheppard RC. Some 'difficult sequences' made easy. A study of interchain association in solid-phase peptide synthesis. *Int. J. Pept. Protein Res.* 1994; **43**: 431–440.
28 Florio T, Paludi D, Villa V, Principe DR, Corsaro A, Millo E, Damonte G, D'Arrigo C, Russo C, Schettini G, Aceto A. Contribution of two conserved glycine residues to fibrillogenesis of the 106–126 prion protein fragment. Evidence that a soluble variant of the 106–126 peptide is neurotoxic. *J. Neurochem.* 2003; **85**: 62–72.
29 Cardona V, Eberle I, Barthélémy S, Beythien J, Doerner B, Schneeberger P, Keyte J, White P. Application of Dmb-dipeptides in the Fmoc SPPS of difficult and aspartimide-prone sequences. *Int. J. Pept. Res. Therapeut.* 2008; **14**: 285–292.
30 Bagley CJ, Otteson KM, May BL, McCurdy SN, Pierce L, Ballard FJ, Wallace JC. Synthesis of insulin-like growth factor I using *N*-methyl pyrrolidinone as the coupling solvent and trifluoromethane sulfonic acid cleavage from the resin. *Int. J. Pept. Prot. Res.* 1990; **36**: 356–361.
31 Varanda LM, Miranda MTM. Solid-phase peptide synthesis at elevated temperatures: a search for an optimized synthesis condition of unsulfated cholecystokinin-12. *J. Pept. Res.* 1997; **50**: 102–108.
32 Auzanneau F-I, Meldal M, Bock K. Synthesis, characterization and biocompatibility of PEGA resins. *J. Pept. Sci.* 1995; **1**: 31–44.
33 Renil M, Meldal M. Synthesis and application of a PEGA polymeric support for high capacity continuous flow solid-phase peptide synthesis. *Tetrahedron Lett.* 1995; **36**: 4647–4650.
34 Renil M, Ferreras M, Delaisse JM, Foged NT, Meldal M. PEGA supports for combinatorial peptide synthesis and solid-phase enzymic library assays. *J. Pept. Sci.* 1998; **4**: 195–210.
35 Kaiser E, Colescott RL, Bossinger CD, Cook PI. Color test for detection of free terminal amino groups in the solid-phase synthesis of peptides. *Anal. Biochem.* 1970; **34**: 595–598.
36 Vazquez J, Qushair G, Albericio F. Qualitative colorimetric tests for solid phase synthesis. *Methods Enzymol.* 2003; **369**: 21–35.
37 Fields CG, Macdonald RL, Otteson KM, Noble RL. HBTU activation for automated Fmoc solid-phase peptide synthesis. *Pept. Res.* 1991; **4**: 95–101.
38 Garcia-Martin F, White P, Steinauer R, Cote S, Tulla-Puche J, Albericio F. The synergy of ChemMatrix resin and pseudoproline building blocks renders RANTES, a complex aggregated chemokine. *Biopolymers* 2006; **84**: 566–575.
39 Cremer G-A, Tariq H, Delmas AF. Combining a polar resin and a pseudo-proline to optimize the solid-phase synthesis of a 'difficult sequence'. *J. Pept. Sci.* 2006; **12**: 437–442.
40 Pastor JJ, Granados G, Carulla N, Rabanal F, Giralt E. Redesign of protein domains using one-bead-one-compound combinatorial chemistry. *J. Am. Chem. Soc.* 2007; **129**: 14922–14932.
41 Atherton ES, Sheppard RC. *Solid Phase Peptide Synthesis: a Practical Approach*. IRL Press: Oxford, 1989.
42 Rabanal F. Base/nucleophile-labile resins (Francesc Rabanal). In *The Power of Functional Resins in Organic Synthesis*, 1st edn, Tulla-Puche J, Albericio F (eds). Wiley VCH Verlag GmbH & Co KGaA: Weinheim, Germany, 2008; 417–436.
43 Kinter M, Sherman NE. *Protein Sequencing and Identification using Tandem Mass Spectrometry*. Wiley-Interscience: New York, 2000.
44 Sreerama N, Woody RW. Computation and analysis of protein circular dichroism spectra. *Methods Enzymol.* 2004; **383**: 318–351.
45 Greenfield NJ. Using circular dichroism spectra to estimate protein secondary structure. *Nat. Protocols* 2007; **1**: 2876–2890.
46 Whitmore L, Wallace BA. Protein secondary structure analyses from circular dichroism spectroscopy: methods and reference databases. *Biopolymers* 2008; **89**: 392–400.
47 Linden R, Martins VR, Prado MAM, Cammarota M, Izquierdo I, Brentani RR. Physiology of the prion protein. *Physiol. Rev.* 2008; **88**: 673–728.
48 Lashuel HA, Hartley D, Petre BM, Walz T, Lansbury PT. Neurodegenerative disease: amyloid pores from pathogenic mutations. *Nature* 2002; **418**: 291.
49 Walsh P, Yau J, Simonetti K, Sharpe S. Morphology and secondary structure of stable beta-oligomers formed by amyloid peptide PrP (106–126). *Biochemistry* 2009; **48**: 5779–5781.
50 Walsh P, Simonetti K, Sharpe S. Core structure of amyloid fibrils formed by residues 106–126 of the human prion protein. *Structure* 2009; **17**: 417–426.

